Bioconjugate Chemistry

pubs.acs.org/bc
Article

An Albumin-Holliday Junction Biomolecular Modular Design for Programmable Multifunctionality and Prolonged Circulation

Anders Dinesen, Veronica L. Andersen, Marwa Elkhashab, Diego Pilati, Pernille Bech, Elisabeth Fuchs, Torbjørn R. Samuelsen, Alexander Winther, Yunpeng Cai, Anders Märcher, Archie Wall, Marjan Omer, Jesper S. Nielsen, Vijay Chudasama, James R. Baker, Kurt V. Gothelf, Jesper Wengel, Jørgen Kjems, and Kenneth A. Howard*

Cite This: *Bioconjugate Chem.* 2024, 35, 214−222
Read Online

ABSTRACT: Combinatorial properties such as long-circulation and site- and cell-specific engagement need to be built into the design of advanced drug delivery systems to maximize drug payload efficacy. This work introduces a four-stranded oligonucleotide Holliday Junction (HJ) motif bearing functional moieties covalently conjugated to recombinant human albumin (rHA) to give a "plug-and-play" rHA-HJ multifunctional biomolecular assembly with extended circulation. Electrophoretic gel-shift assays show successful functionalization and purity of the individual high-performance liquid chromatography-purified modules as well as efficient assembly of the rHA-HJ construct. Inclusion of an epidermal growth factor receptor (EGFR)-targeting nanobody module facilitates specific binding to EGFR-expressing cells resulting in approximately 150-fold increased fluorescence intensity determined by flow cytometric analysis compared to assemblies absent of nanobody inclusion. A cellular recycling assay demonstrated retained albumin-neonatal Fc receptor (FcRn) binding affinity and accompanying FcRn-driven cellular recycling. This translated to a 4-fold circulatory half-life extension (2.2 and 0.55 h, for the rHA-HJ and HJ, respectively) in a double transgenic humanized FcRn/albumin mouse. This work introduces a novel biomolecular albumin-nucleic acid construct with extended circulatory half-life and programmable multifunctionality due to its modular design.

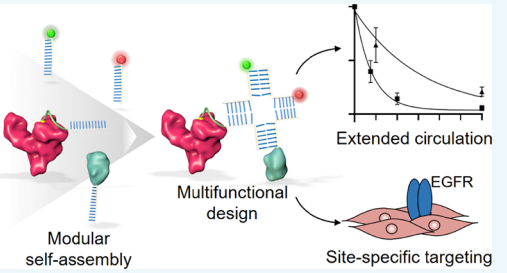

1. INTRODUCTION

Temporal, spatial, and quantal control in drug delivery are crucial to maximize efficacy and minimize side-effects, but achieving the required long circulation, site-specificity, and drug payload levels is a challenge. Combinatorial properties incorporated into a single drug delivery design is highly desirable.[1] The use of nucleic acid nano-scaffolds comprising of functionalized oligonucleotide modules is an attractive strategy for producing multifunctional drug constructs. This approach allows *plug-and-play* assembly to control the type, stoichiometry, and spatial arrangement of functional moieties. The therapeutic utility of naked nucleic acids, however, is limited by poor stability and a short circulatory half-life *in vivo*.[2,3]

Albumin is a transport protein with a long circulatory half-life of approximately 19 days in humans[4,5] facilitated by interaction with the cellular FcRn.[6] This occurs by a pH-dependent endosomal sorting pathway redirecting albumin from lysosomal degradation and allows recycling and release at the cell surface.[6,7] Furthermore, albumin has a broad tissue distribution and has been shown to accumulate at tumor sites.[8,9] This promotes albumin as an attractive carrier for functional nano-scaffolds particularly in cancer therapeutics.

Utilization of albumin for half-life extension can be achieved by non-covalent binding to endogenous albumin through fatty acid modification, but this non-site-specific approach is susceptible to displacement by endogenous ligands and offers little control over attachment stoichiometry and can lower bioactivity of both components by sub-optimal placement. Specifically, non-site-specific association at the main binding interface of FcRn in albumin Domain III can lead to interference in FcRn-mediated half-life extension. Covalent conjugation to albumin's single free thiol at cysteine 34 (Cys34) in albumin domain I, distant from the main albumin-FcRn binding interface,[12] offers stoichiometrically defined and site-selective conjugation at a site that minimizes interference with FcRn binding.

We have previously introduced a conjugated albumin-oligonucleotide modular assembly based on a simple oligonucleotide duplex design to incorporate aptamers,[10] fluorophores,[10,11] and cytotoxic drug molecules.[11] This was

Received: November 10, 2023
Revised: December 22, 2023
Accepted: December 22, 2023
Published: January 17, 2024

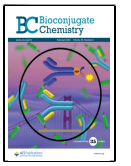

https://doi.org/10.1021/acs.bioconjchem.3c00491
Bioconjugate Chem. 2024, 35, 214−222

performed by annealing a functionalized oligonucleotide module to a complementary oligonucleotide site-selectively conjugated to Cys34. Whilst, conjugation to both the 5′ and 3′ terminal of the duplex assembly can accommodate up to three functional moieties, possible inter-moiety steric hindrance in the duplex may occur. Therefore, more elaborate oligonucleotide structures that ensure adequate spatial separation of functionalities are an attractive approach.

Andersen et al. have designed and investigated a four stranded Holliday Junction (HJ) where all four intercomplementary oligonucleotide modules (Q1−Q4) carry a 5′-handle for conjugation of functional moieties allowing modular assembly of up to four functionalities.[13] Importantly, the 4 nm junctional design ensures radial display of the termini tethered functionalities to minimize steric hindrance within the assembly. The HJ assembly is, however, susceptible to rapid renal clearance and a limited tissue distribution.

In this work, we have integrated the HJ into our previously described recombinant human albumin (rHA)-oligonucleotide design by site-selective conjugation of one of the HJ strands to Cys34 of rHA, which acts as a scaffold for subsequent HJ self-assembly following the addition of the three remaining functionalized HJ strands.

rHA-HJ assembly and programmable functionality are exemplified by incorporation of an epidermal growth factor receptor (EGFR)-targeting nanobody (EgA1 clone) module in combination with two different fluorophore modules (Figure 1). These were selected as a proof-of-concept theranostic

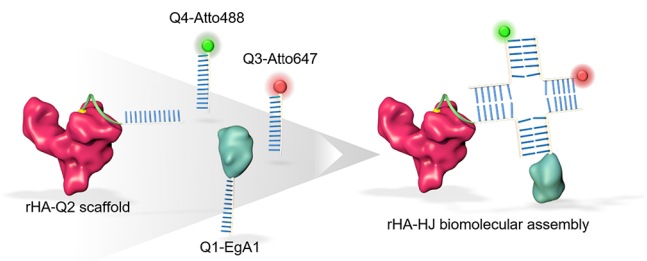

Figure 1. Schematic representation of the functionalized rHA-HJ biomolecular design formed by the annealing of complementary oligonucleotide modules (Q1, Q3, and Q4) to the rHA-oligonucleotide (Q2) scaffold. The green line represents the linker connecting Q2 to albumin and the white ribbon with blue sticks represent the oligonucleotide modules Q1, Q3, and Q4 functionalized with anti-EGFR nanobody (EgA1), Atto647, or Atto488 fluorophores, respectively.

design as binding of EGFR, a validated target for several types of tumor cells, can afford a therapeutic effect through signal transduction inhibition, while inclusion of fluorophores can potentially be used to track of EGFR-positive disease location and progression.

2. RESULTS

2.1. Production of the Albumin-Holliday Junction Biomolecular Assemblies. The four strands of the HJ (Q1−Q4) were functionalized and purified individually, and the modules were then self-assembled by complementary base pair annealing to form the rHA-HJ biomolecular assembly.

2.1.1. Production of the rHA-Q2 Scaffold. We have previously used a standard maleimide linker for attachment of a 21-mer DNA strand to Cys34 of albumin.[10] However, utilizing this for conjugation of the shorter and highly modified 12-mer Q2 oligonucleotide strand presented issues in the ion-exchange (IEX)-HPLC purification, with excess unconjugated oligonucleotides overlapping with the rHA-Q2 conjugate peak (Figure S1), resulting in poor annealing efficiency of the rHA-HJ assembly (data not shown). The conjugation and purification was improved by employing a recently published stable monobromomaleimide (MBM)-bicyclo[6.1.0]nonyne (BCN) linker,[11] which afforded pure rHA-Q2 fractions (Figure 2 fraction 1−7 pooled in frame C).

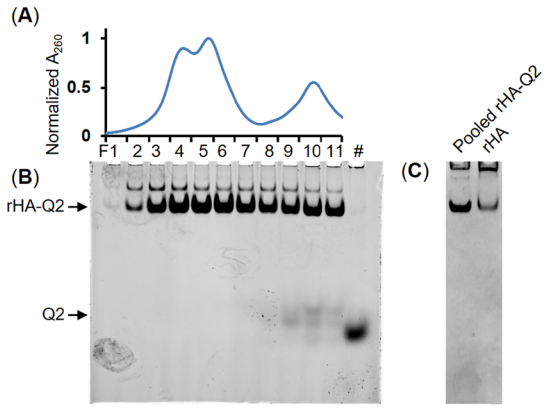

Figure 2. Purification of rHA-Q2. (A) Cutout of the IEX-HPLC chromatogram showing absorbance at 260 nm indicating the oligonucleotide. The fraction number is shown below the chromatogram. (B) SYBR gold stained native PAGE gel of fraction 1−11 of the corresponding IEX-HPLC purification as shown above. # indicates a Q2 control lane. (C) Coomassie blue stained native PAGE gel of the pooled purified product consisting of the fractions free of excess free Q2 oligonucleotide (fraction 1−7 in frames (A) and (B)).

2.1.2. Production of the Q1-Anti-EGFR Nanobody (EgA1) Module. The EgA1 nanobody[14,15] with a 4-azido-L-phenylalanine unnatural amino acid (UAA) incorporated close to the C-terminal allowed conjugation to dibenzocyclooctyne (DBCO)-functionalized oligonucleotides without affecting the target binding of the nanobody.[16] The EgA1-UAA was expressed and purified with a final yield of 700 μg/L culture. SDS-PAGE analysis revealed an expected main band around 15 kDa with a purity of >80% determined by Coomassie Blue staining (Figure 3A).

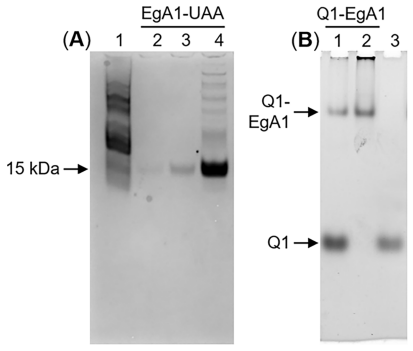

Figure 3. EgA1-UAA expression and oligonucleotide conjugation. (A) Coomassie stained SDS-PAGE gel. Lane 1: Molecular weight ladder, lanes 2, 3, and 4 are 10, 20, and 100 pmol of purified EgA1-UAA, respectively. (B) SYBR gold stained native PAGE gel. Lane 1: Unpurified Q1-EgA1 conjugate; lane 2: Gel purified Q1-EgA1 conjugate, lane 3: Q1 oligonucleotide control.

https://doi.org/10.1021/acs.bioconjchem.3c00491
Bioconjugate Chem. 2024, 35, 214−222

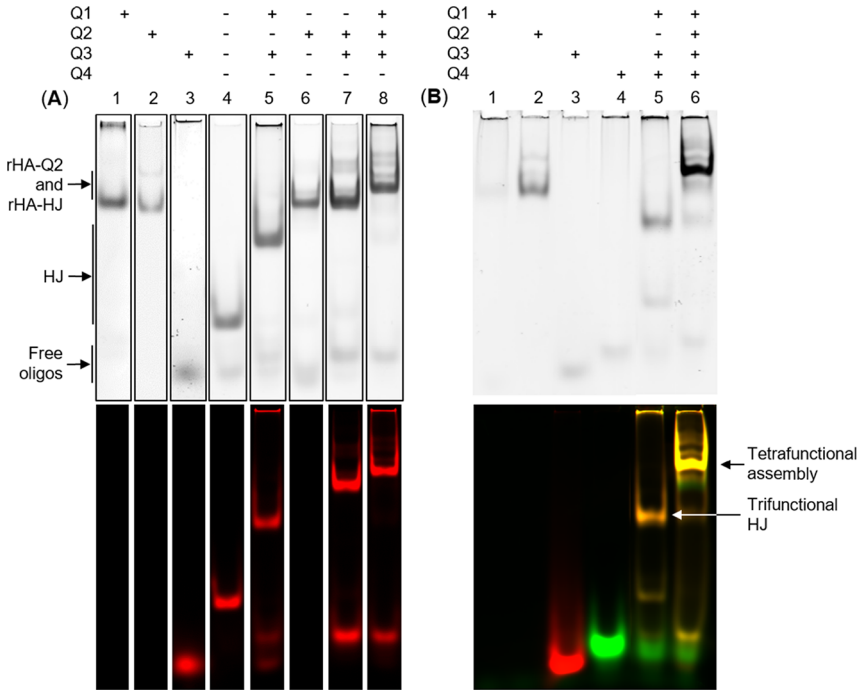

Figure 4. Formation of biomolecular assemblies visualized with native PAGE. (A) Lane 1: Q1-EgA1 control; lane 2: rHA-Q2 control; lane 3: Q3-Atto647 control, lane 4: HJ(Atto647), lane 5: HJ(EgA1, Atto647), lane 6: rHA-HJ, lane 7: rHA-HJ(Atto647), and lane 8: rHA-HJ(EgA1, Atto647). (B) Lane 1: Q1-EgA1 control, Lane 2: rHA-Q2 control, lane 3: Q3-Atto647 control, lane 4: Q4-Atto488 control, lane 5: HJ(EgA1, Atto647, Atto488), lane 6: rHA-HJ(EgA1, Atto647, Atto488). Black bands: SYBR gold signal; red bands: Atto647 signal, green bands: Atto488 signal, yellow bands: Overlap of the Atto647 and Atto488 signals. In the lane legend, "-" indicates presence of the corresponding non-functionalized strand (Q1−4) and "+" indicates functionalized strands (Q1-EgA1, rHA-Q2, Q3-Atto647, and Q4-Atto488).

The EgA1-UAA was conjugated to DBCO-functionalized Q1 oligonucleotide and gel purified to give Q1-EgA1 free of excess oligonucleotide and nanobody, as shown by Native PAGE (Figure 3B) and IEX-HPLC (Figure S2), respectively.

2.1.3. Annealing of Functionalized rHA-HJ Biomolecular Assembly. Assembly of the HJ was successful with both non-functionalized and functionalized strands (Figure 4). The inclusion of an EgA1 nanobody on the Q1 strand in the assembly resulted in an upward band-shift (Figure 4A, lanes 5 and 8), while incorporation of Atto647 on the Q3 strand was confirmed by colocalization of its fluorescence with the assembled HJ and rHA-HJ (Figure 4A, lanes 4, 5, 7, and 8). Efficient annealing was shown, with more than 80% of the SYBR gold signal coinciding with the assembled construct (top bands in Figure 4A, lane 4−8). The inclusion of an Atto488 fluorophore on the Q4 strand, in addition to inclusion of albumin, EgA1, and Atto647, was used to demonstrate the ability to occupy all modules with functionalities. The tetrafunctional assembly is visualized by a yellow band indicating colocalization of the Atto647 and Atto488 signals (Figure 4B lane 6).

2.2. Cellular EGFR Binding of Biomolecular Assemblies. Cellular EGFR-targeting by incorporation of an EgA1 nanobody into the biomolecular design was evaluated in EGFR negative (3T3) and positive (3T3-EGFR and A431) cell lines (Figure 5). The HJ and rHA-HJ assemblies were functionalized with Atto647 to visualize the cellular interaction by flow cytometry. All assemblies incorporating the EgA1 nanobody exhibited strong binding to EGFR-expressing cells with HJ(EgA1, Atto647), displaying 160- and 200-fold increased cell fluorescence intensity over non-targeted HJ(Atto647) in 3T3-EGFR and A431 cells, respectively. Similarly, rHA-

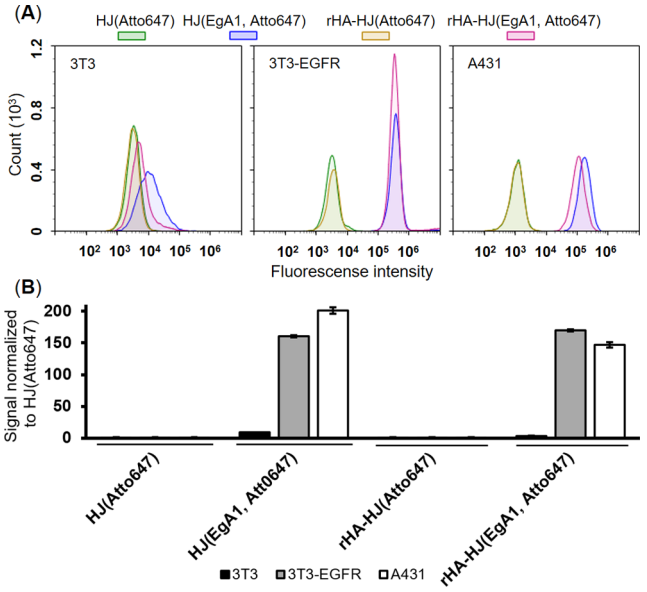

Figure 5. Flow cytometric analysis showing levels of biomolecular assembly binding to EGFR negative 3T3 cells and EGFR positive 3T3-EGFR and A431 cells. (A) Representative chromatograms showing Atto647 fluorescence intensity in the three cell lines. (B) Quantitation of mean cell fluorescence relative to HJ(Atto647). $N = 3$ independent experiments; error bars indicate SD.

HJ(EgA1, Atto647) increased fluorescence 170- and 150-fold binding to 3T3-EGFR and A431 cells compared to non-targeted HJ(Atto647), respectively (Figure 5B). In the 3T3 cells, incorporation of the nanobody afforded a very slight increase in fluorescence compared to non-targeted assemblies

https://doi.org/10.1021/acs.bioconjchem.3c00491
Bioconjugate Chem. 2024, 35, 214−222

that could reflect a low level of EGFR expression. These observations match the EGFR expression levels of the respective cell lines determined by flow cytometry using an anti-EGFR antibody, cetuximab, that showed similar and high EGFR expression for 3T3-EGFR and A431 cells and very low levels in the 3T3 cell line (see Figure S3). Taken together, we demonstrate EGFR-specific cellular association by incorporating the EgA1 nanobody into the biomolecular design that offers the potential for cellular drug targeting.

2.3. FcRn-Mediated Cellular Recycling and Half-Life Extension of Biomolecular Assemblies. The interaction of FcRn with the albumin component of the biomolecular assemblies was evaluated in a cellular recycling assay in which FcRn overexpressing cells are incubated with the assemblies and the amount recycled back into fresh media due to FcRn-mediated recycling was measured (Figure 6). The

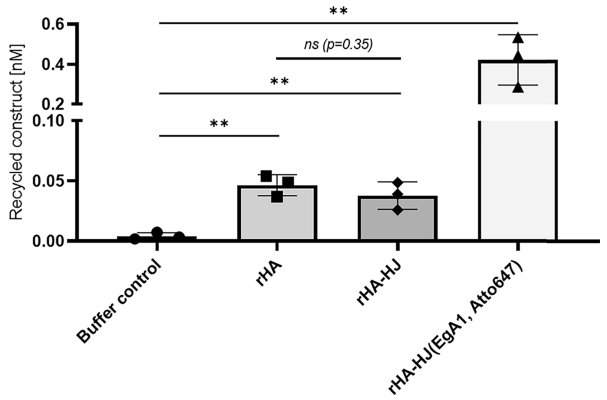

Figure 6. ELISA quantitation of FcRn-mediated cellular recycling of albumin biomolecular assemblies after incubation with FcRn-transduced human microvascular endothelial cell line-1 (HMEC-1-FcRn) cells. Buffer control is an albumin-free negative control. $N = 3$ independent experiments; error bars indicate standard deviation (SD). Statistics were performed using Student's t test, $^{**}p < 0.01$.

rHA control showed similar recycling levels to our previously published work[6] while a buffer control exhibited minimal signal. Importantly, the recycling of rHA-HJ was not significantly different from the recycling of rHA alone ($p = 0.35$) confirming minimal interference by the oligonucleotide assembly with albumin's FcRn engagement. Interestingly, the functionalized rHA-HJ(EgA1, Atto647) assembly was recycled to 9-fold higher levels compared with rHA alone (Figure 6). These results demonstrate maintained FcRn engagement of the albumin component of the biomolecular assemblies with additional effects leading to increased recycling for the functionalized assembly.

The stability of the construct was confirmed by Native PAGE following incubation in 10% human serum at 37 °C, where no evident degradation was observed over the 90 h time period investigated (Figure S4). Subsequently assemblies containing a far red fluorophore, Cy5.5, were used to investigate the circulatory half-life of HJ(EgA1, Cy5.5) and rHA-HJ(EgA1, Cy5.5) in a double transgenic mouse homozygous for human albumin and FcRn[17] (Figure 7). The functionalized HJ alone exhibited a half-life of 0.55 h, whilst, the HJ on the rHA scaffold (rHA-HJ) resulted in a 4-fold extension of the circulatory half-life to 2.2 h.

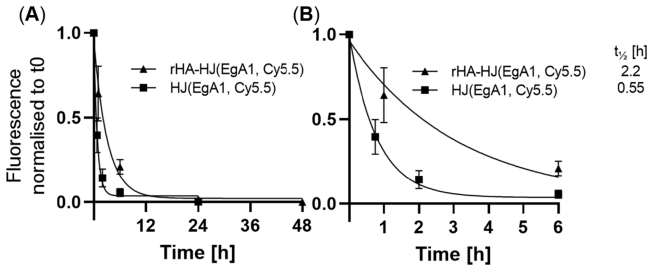

Figure 7. Circulatory half-lives of rHA-HJ(EgA1, Cy5.5) and HJ(EgA1, Cy5.5). Fluorescence intensity was measured and normalized to t_0 in blood taken at indicated time points. (A) Data in blood collected over 48 h. (B) Data in blood collected from time 0−6 h. $N = 4$ mice per group.

3. DISCUSSION

Combinatorial properties incorporated into a single drug delivery design with the versatility to *plug-and-play* with functional modules are highly desirable. In this work, we introduce a multifunctional rHA-HJ biomolecular assembly with the potential for FcRn-driven prolonged circulation and incorporation of functionalized oligonucleotide modules exemplified with an anti-EGFR nanobody and two different fluorophores.

We have previously introduced an albumin-oligonucleotide platform incorporating aptamers, cytotoxic drugs, or fluorophores using a simple oligonucleotide duplex design.[10,11] The attachment site of the oligonucleotide at albumin's Cys34 is crucial to avoid interference with albumin's FcRn interaction and, thereby, retain the accompanying FcRn-driven cellular recycling.[6] The duplex design may, however, offer limited spatial separation and display of functional groups, providing the rationale for introducing the novel rHA-four-stranded HJ assembly in this work. The 4 nm HJ configuration ensures a spatial distance and radial display of functional groups at the termini of the oligonucleotide modules (Q1, 3, and 4) following assembly onto an albumin-oligonucleotide (Q2) scaffold.

The Q2 oligonucleotide was conjugated to rHA using a recently published MBM-BCN linker.[11] The MBM is an improved thiol-reactive chemistry compared to conventional maleimide, as it does not undergo retro-Michael cleavage after conjugation and, in addition, affords faster stabilizing hydrolysis under milder conditions.[18,19] In this work, we observed more efficient conjugation and purification when using the MBM linker system compared with a conventional SM(PEG)$_8$ maleimide-based linker (Figure S1). The conjugation yield is expected to increase through prevention of the retro-Michael cleavage, while it is speculated that the improved purification is a result of different interactions between the IEX column and the tetrazine-modified oligonucleotide, used for the MBM conjugation compared to the traditional SM(PEG)$_8$-linker.

A cellular recycling assay, shown by our group to be an excellent predictor of *in vivo* half-life of albumin-based therapeutics,[20] revealed that both non-functionalized and functionalized rHA-HJ underwent FcRn-mediated cellular recycling in HMEC-1-FcRn cells. Increased recycling was observed for EgA1 and Atto647 functionalized assemblies compared to the non-functionalized designs. We have previously also observed increased cellular recycling of a fluorophore functionalized albumin-duplex assembly.[11] It is

https://doi.org/10.1021/acs.bioconjchem.3c00491
Bioconjugate Chem. 2024, 35, 214−222

Table 1. Oligonucleotide Sequences and Modifications (Blue = 2′*O*-Me, Red = LNA)

Oligonucleotide ID	5′ modification	Sequence (5′ to 3′)
Q1	C_6-NH_2	CCG TCC TGA GCC
Q2	C_6-NH_2	CAC AGT GGA CGG
Q3	C_6-NH_2	GGC TCA CCG ATC
Q4	C_6-NH_2	GAT CGG ACT GTG

speculated that the inclusion of fluorophores could mediate hydrophobic interactions with the cell membrane and that these additional cellular interactions could increase the internalization and subsequent recycling of the functionalized construct. Furthermore, our previous work has shown increased recycling of albumin-EGFR fusion proteins through possible additional binding to EGFR expressed on HMEC-1-FcRn cells.[20]

Circulatory half-life evaluation revealed a 4-fold half-life extension of the rHA-HJ (2.2 h) compared to naked HJ (0.55 h) in the double transgenic human FcRn/human albumin mouse. This model allows an autologous receptor/ligand interaction and, therefore, a more human physiologically relevant model to evaluate human albumin-based drugs[17] than traditional models.[21] It may be expected that HJ inclusion onto a rHA scaffold would mediate a longer half-life than the observed 2.2 h, but competition for FcRn from the endogenous human albumin pool and cellular interactions of the HJ component could influence pharmacokinetics. Previous work with the HJ construct showed similar circulatory half-life (2.7 h) with the addition of two PEG moieties[13]; however, concerns about PEG immunogenicity[22] promotes rHA as an attractive alternative half-life technology.

Andersen et al. functionalized an HJ with fatty acids to non-covalently bind to endogenous albumin that prolonged the half-life to just over 2 h.[13] The Cys34 site-specific covalent conjugation approach used in our work offers conjugation at a defined site on albumin limiting possible interference with FcRn binding that may occur with non-site-specific association. In addition, the availability of recombinant albumin variants with engineered FcRn affinity offers tunable circulatory half-life[23] that we have demonstrated with albumin genetic fusions.[20,24] Furthermore, covalent conjugation is not susceptible to competition and displacement from other albumin binding ligands observed with non-covalent drug association.

The HJ is composed exclusively from the stabilized nucleic acid analogues locked nucleic acids (LNA)[25,26] and 2′-*O*-methyl modified nucleotides (2′*O*-Me) showed high stability and prevented degradation in 10% human serum. Previous work using a two-strand system showed high stability even in 50% serum.[11] However, disassembly of the annealed HJ construct under physiological conditions *in vivo* cannot be discounted and may have contributed to the shorter than expected half-life extension, as discussed above. Future work could address inclusion of other stabilized nucleotide analogues or different sizes and architectures of the assembly.

The synthesis of the LNA utilized in this work requires 15 chemical steps, and therefore, alternative nucleic acid analogues are being developed. Recently, Märcher et al. published an acyclic (L)-threoninol nucleic acid ((L)-aTNA) junction for which the phosphoramidites can be synthesized in 5−10 steps[27] Similar to this work, the (L)-aTNA junction was functionalized with a nanobody and exhibited targeting to cells expressing a cancer biomarker.[27]

EGFR is commonly overexpressed in cancers, therefore, serving as a candidate for tumor targeting.[28] Flow cytometric analysis showed retained functionality of the anti-EGFR nanobody after inclusion into the biomolecular assemblies by exhibiting EGFR-specific binding in the EGFR-overexpressing cells compared to the EGFR low expressing cells. FcRn, shown to be overexpressed in cancer tissue, may also afford greater accumulation in cancer tumor tissue using albumin-based drug designs.[9,29] Furthermore, in addition to the tumor targeting, the binding epitope of EgA1 on EGFR prevents receptor dimerization, which is necessary for signal transduction, and EgA1 and EgA1-containing constructs can, therefore, act to inhibit tumor proliferation.[15]

The modular design of the rHA-HJ assembly offers the capability to multiplex targeting moieties. Multivalent or multi-epitope binding is expected to synergistically improve targeting of the assembly through avidity effects. EGFR is active as a dimer with a distance between the EgA1 binding sites of ∼5 nm[15,30] comparable with the 4 nm dimensions of the HJ[13] possibly allowing avidity-increased binding strength by incorporating two EgA1 nanobodies in the rHA-HJ design, which constitutes a promising direction for future work.

4. CONCLUSIONS

This work introduces a novel albumin-HJ biomolecular assembly with modular multifunctionality, exemplified by incorporation of an EGFR-targeting nanobody and fluorophores. Furthermore, the assembly retains FcRn engagement that translates to an extended circulatory half-life compared to that of the naked HJ. The ability to plug-and-play with different functional modules underscores design versatility. The design accommodates assembly of constructs with multiple targeting and drug moieties, allowing potential synergistic effects in targeting through avidity and in efficacy by increased drug-to-albumin ratio or combinatorial drug action.

5. EXPERIMENTAL SECTION

5.1. Materials. rHA expressed in *S. cerevisiae* was obtained from Sigma-Aldrich (cat# A6608).

The sequence and modifications of the oligonucleotides used are listed in Table 1.

5.2. Cell Lines and Cell Culture. Cell lines were cultured at 37 °C and 5% CO_2.

HMEC-1-FcRn cells previously generated[6] were cultured in MCDB 131 medium (Life Technologies, cat# 10372−019) with 10 ng/mL human epidermal growth factor (Peprotech, cat# AF-100−15), 1 μg/mL hydrocortisone (Sigma, cat# H0888), 50 μg/mL Geneticin (Gibco, cat# 10131−035), 0.25 μg/mL Puromycin (Life Technologies, cat# A11138−03), 2 mM L-glutamine (Lonza, cat# BE17−605E), and 10% fetal bovine serum (FBS, Gibco, cat# 10500−064).

3T3, 3T3-EGFR, and A431 cells were cultured in Dulbecco's modified eagle medium (DMEM, Gibco cat#

https://doi.org/10.1021/acs.bioconjchem.3c00491
Bioconjugate Chem. 2024, 35, 214−222

41966−029) supplemented with 10% FBS and 1% penicillin/streptomycin (P/S) (Gibco, cat# 14140−122).

5.3. EgA1 Expression and Purification. The sequence for the EgA1 was modified with a C-terminal amber stop codon for incorporation of the UAA 4-azido-L-phenylalanine adopting the approach of Chatterjee et al.,[31] followed by a hexa-histidine-tag and cloned into a pET-22b(+) vector for expression and purification similar to Teodori et al.[16] Briefly, BL21 *E. coli* were transformed with the pET-22b(+) and pULTRA plasmids by heat shock and cultured on 2xYT agar plates (16 g/L tryptone, 10 g/L yeast extract, 5 g/L NaCl, and 15 g/L agar) with 100 μg/mL of both ampicillin and spectinomycin selection overnight at 37 °C. A single colony was used to inoculate a starter culture of 4 mL of TB medium (24 g/L yeast extract, 12 g/L tryptone, and 0.45% glycerol) with 72 mM K_2HPO_4, 17 mM KH_2PO_4, 2 mM MgCl2, 0.1% glucose, and 100 μg/mL of both ampicillin and spectinomycin and cultured overnight at 37 °C with 200 rpm orbital shaking. The starter culture was transferred to 800 mL of fresh medium and grown to an OD_{600} of 0.6−0.9 before induction by adding isopropyl β-D-1-thiogalactopyranoside (IPTG) and UAA to end concentrations of 1 mM and 2 g/L, respectively, and cultured overnight at 28 °C with 200 rpm orbital shaking.

Periplasmic extraction was performed by centrifugation (4500 rpm, 30 min, + 4 °C), suspension in 12 mL cold 4× TES buffer (0.2 M tris, 0.5 mM EDTA, 0.5 M sucrose, pH 8), incubating 1 h at +4 °C with 20 rpm inversion. Twenty-four mL of 1× TES buffer was added, and incubation was repeated before centrifugation (9000*g*, 30 min, +4 °C) and sterile filtering of the supernatant using a 0.22 μm poly(ether sulfone) (PES) filter (Corning, cat# 431097).

Ni-NTA purification was performed with a kta Start (Cytiva, Marlborough, USA) on a HisTrap Excel 1 mL column (Cytiva, cat# 17−3712−05) with the following program at 1 mL/min: 5 CV equilibration with buffer A (20 mM NaH_2PO_4, 0.5 M NaCl, pH 7.4), sample application, and 10 CV washing with buffer A. The produced nanobody was eluted with a 10 CV gradient from 0% to 100% buffer B (20 mM NaH_2PO_4, 0.5 M NaCl, 1 M imidazole, pH 7.4) and an additional 5 CV of buffer B before washing with 10 CV buffer A. The sample was concentrated and buffer exchanged to Dulbecco's phosphate buffered saline (DPBS, Sigma, cat# D8537) by ultracentrifugation through a 3 kDa cutoff filter (Merck, cat# UFC500396).

5.4. Oligonucleotide Functionalization and Annealing. *5.4.1. Oligonucleotide Conjugation to EgA1.* NHS-ester-DBCO linker (Sigma, cat# 761524) (750 nmol, 50 equiv) in dimethyl sulfoxide (DMSO, 7.5 μL) was conjugated to Q1 oligonucleotide (15 nmol, 1.0 equiv) in 15 μL of nuclease-free water (NFW, Invitrogen, cat# AM9937) with 75 μL of DMSO and 112.5 μL of 0.1 M 4-(2-hydroxyethyl)-1-piperazineethanesulfonic acid (HEPES) pH 8.0 and incubated overnight at room temperature (RT) with 650 rpm orbital shaking. Ethanol precipitation (Section 5.4.4) removed the excess linker. Q1-DBCO (∼15 nmol, 1.0 equiv) in 20 μL of NFW and Q1 conjugated to EgA1-azide (30 nmol, ∼2 equiv) in 190 μL of DPBS by incubating overnight at RT with 650 rpm orbital shaking.

Gel purification was performed by running the conjugate on an 8% native PAGE gel and staining with SYBR gold (as described in section 5.5, using a larger gel and run for 1 h at 200 V). Imaging allowed localization of the conjugate band, which was excised and cut into ∼1 mm pieces and incubated in NFW overnight at 4 °C with tube rotation. The liquid was extracted using Freeze N' squeeze DNA gel extraction spin columns (Bio-Rad, cat# 7326165) according to the manufacturer's instructions, followed by concentration and buffer exchange to DPBS by ultracentrifugation through a 3 kDa cutoff filter.

5.4.2. Oligonucleotide Conjugation to rHA. Q2 was conjugated to rHA by modifying the oligonucleotide with a tetrazine for conjugation to rHA modified with an MBM-BCN linker.

Tetrazine-$(PEG)_5$-NHS-ester linker (BroadPharm, cat# BP-22681) (500 nmol, 50 equiv) in 5 μL of DMSO was conjugated to Q2 oligonucleotide (10 nmol, 1.0 equiv) in 10 μL of NFW with 15 μL of DMSO and 30 μL of 0.1 M HEPES pH 8.0 and incubated overnight at RT with 650 rpm orbital shaking. Ethanol precipitation (Section 5.4.4) was used to remove excess linker.

MBM-BCN linker (100 nmol, 5.0 equiv) in 10 μL of DMSO was conjugated to rHA (20 nmol, 1.0 equiv) in 190 μL with 0.1 M HEPES pH 7.0 for 15 min at RT with 650 rpm orbital shaking. Ultracentrifugation through a 10 kDa cutoff filter (Merck, cat# UFC501096) removed excess linker. Recovered rHA-BCN (∼20 nmol, 1.0 equiv) in ∼35 μL of 0.1 M HEPES pH 7.0 was conjugated to (10 nmol, ∼0.5 equiv) tetrazine-modified Q2 oligonucleotide in 20 μL of NFW overnight at RT with 650 rpm orbital shaking. Conjugate hydrolysis was achieved by adding a 9-fold volumetric excess of 0.1 M HEPES pH 8.0 and incubating at 37 °C for at least 6 h with 650 rpm orbital shaking, followed by purification with IEX-HPLC (Section 5.4.5).

5.4.3. Oligonucleotide Conjugation to Atto647 and Atto488 Fluorophores. Atto647- and Atto488-NHS-ester linkers (125 nmol, 25 equiv) in 10 μL of DMSO were conjugated to Q3 and Q4 oligonucleotides (5 nmol, 1.0 equiv) in 5 μL of NFW with 300 μL of DMSO and 35 μL of 0.1 M HEPES pH 8.2 with incubation overnight at RT with 750 rpm orbital shaking. Ethanol precipitation (Section 5.4.4) removed the excess linker before purification with ion-pair reversed-phase (IP-RP) HPLC using a C18 column (Section 5.4.5).

5.4.4. Ethanol Precipitation. Modified oligonucleotide (12.5%), absolute ethanol (EtOH, VWR, cat# 20821.310) (77.5%), and 3 M sodium acetate (NaOAc, Sigma, cat# S2889) (10%) were incubated at −20 °C for 3 h and centrifuged (17,000*g*, 45 min). After aspiration, the pellet was washed with EtOH, centrifuged (17,000*g*, 30 min), aspirated, and dried for 10 min before dissolving in NFW.

5.4.5. HPLC Purification. HPLC purification was performed on a system consisting of a low-pressure gradient (LPG)-3400RS pump, variable wavelength detector (VWD)-3400RS, and Ultimate 3000 automated fraction collector (AFC, Thermo Fisher Scientific). After filtering with a 0.2 μm polypropylene (PP) filter (Kinesis, cat# ESF-PP-04−022), samples were injected into a Rheodyne 9725i manual injector (Thermo Fisher Scientific) with a 500 μL polyether ether ketone (PEEK) sample loop using a 100 μL Hamilton syringe (Sigma-Aldrich).

Preparative IEX chromatography was performed with a Mono Q 5/50 GL anion exchange column (Cytiva, cat# 17516601) at 0.3 mL/min with a 25 min gradient from 100% buffer A (20 mM Tris (Sigma, cat# T5941) and 10 mM NaCl (Acros Organics, cat# 207790010) at pH 7.6), to 100% buffer B (20 mM Tris and 800 mM NaCl at pH 7.6) followed by 5 min of only buffer B. The relevant fractions were desalted and

https://doi.org/10.1021/acs.bioconjchem.3c00491
Bioconjugate Chem. 2024, 35, 214−222

concentrated by centrifugation through 10 kDa molecular weight cutoff filters.

Preparative IP-RP chromatography was performed with an XTerra MS C18 column (Waters) at 0.5 mL/min with a 20 min gradient from 100% buffer A (5% triethylammonium acetate (TEAA, Sigma, cat# 69372) and 5% acetonitrile (MeCN, VWR, cat# 83639.320) in Milli-Q water) to 100% buffer B (100% MeCN) followed by 5 min of only buffer B. The relevant fractions were dried using an RVC 2−18 speed vacuum centrifuge (Martin Christ) before resuspension in NFW.

5.4.6. Annealing of Functionalized Oligonucleotides. For oligonucleotide annealing to the rHA-Q2 scaffold, equimolar amounts of complementary strands (Q1, 3 and 4) were mixed in 200 mM potassium acetate (KOAc, Sigma, cat# P1190) incubating at RT for 4 h.

A total of 260 nm absorbance was used to determine oligonucleotide concentrations, compensating for fluorophore absorbance at 260 nm by a correction factor (CF_{260}): CF_{260}(Atto647) = 0.08 and CF_{260}(Atto488) = 0.22. The bicinchoninic acid (BCA) assay (Thermo Scientific, catalog no. 23225) was performed according to the manufacturer's instructions to determine rHA-Q2 concentration.

5.5. Gel Electrophoresis of Functionalized Oligonucleotides and Biomolecular Assemblies. 8% native PAGE gels were casted by mixing 5 mL of ProtoGel (National Diagnostics, cat# EC-890), 4 mL of Milli-Q water, 1 mL of 10× tris, borate, and ethylenediamine tetraacetic acid (TBE, Thermo Fisher Scientific, cat# 15581−044), 100 μL 10% ammonium persulfate (APS, Sigma, cat# A3678), and 10 μL *N*,*N*,*N*′,*N*′-tetramethylethylenediamine (TEMED, Sigma, cat# T9281) and polymerized for 45 min in 1 mm cassettes (Invitrogen, cat# NC2010) with a 10 or 12-well comb (Invitrogen cat# NC3010 or NC3012).

Samples for native PAGE were mixed with loading buffer to an end concentration of 10% glycerol (VWR, cat# 24388.295) and 1 g/L Orange G (Sigma, cat# O3756). Gels were run in a TBE buffer at 150 V for 30 min with an electrophoresis power supply (EPS) 601 (Amersham Biosciences).

Nucleic acids were stained with SYBR Gold (Invitrogen, catalog no. S11494) according to the manufacturer's instructions. Fluorescence imaging was performed with an Amersham Typhoon 5 (Cytiva).

10% sodium dodecyl sulfate (SDS) polyacrylamide gel electrophoresis (PAGE) gels were casted by mixing 3.4 mL of ProtoGel, 4 mL of Milli-Q water, 2.8 mL of 1.5 M Tris pH 8.7, 138 μL of 10% SDS (Sigma, cat# L4509), 77.5 μL of 10% APS, and 6.9 μL of TEMED and polymerized similarly to native gels.

SDS-PAGE samples were mixed with reducing agent and loading buffer (Invitrogen, cat# NP0009 and NP0007) and heated at 95 °C for 5 min before loading alongside a PageRuler Plus prestained (Thermo Scientific, cat# 26619) protein ladder and run in 3-(*N*-morpholino)propanesulfonic acid (MOPS, Invitrogen, cat# NP0001) buffer. Gels were run at 125−150 V for 75−120 min at RT.

Coomassie staining was performed using 0.3 g/L Coomassie Brilliant Blue (Sigma, catalog no. B7920) in 4.5% methanol (Sigma, catalog no. 34860) and 1% acetic acid (Merck, catalog no. 101830) for 20 min with orbital shaking. Destaining was performed in 10% methanol and 7.5% acetic acid as needed. Imaging of Coomassie stained gels were performed with a Gel Doc EZ Imager (BioRad).

5.6. FcRn-Mediated Cellular Recycling Assay. FcRn-mediated cellular recycling of rHA and the biomolecular assemblies was investigated using the method developed by Schmidt et al.[6] with culturing at 37 °C, 5% CO_2. 100,000 cells were cultured in a 48-well plate (Sarstedt, cat# 83.3923) precoated with Geltrex using thin layer method (Life Technologies, cat# A1413202) until near confluent. The cells were then washed and incubated for 1 h with 300 μL of 150.4 nM of the sample in Hank's balanced salt solution (Sigma, cat# H9269) with MES buffer (Sigma, cat# M1317) at pH 6.0. The cells were washed with cold DPBS and then incubated for 1 h with 160 μL of serum-free medium, in which the recycled sample concentration was quantified by sandwich ELISA:

96-well plates (Thermo Scientific, catalog no. 442404) coated with antialbumin capture antibody (Sigma, catalog no. A7544) for 2 h at RT were blocked with DPBS supplemented with 2% skimmed milk powder (Sigma, catalog no. 70166) for 2 h at RT before incubation with recycled samples and corresponding dilution series overnight at +4 °C. The plates were then incubated with an HRP-conjugated antialbumin antibody (Abcam, catalog no. 19183) for 2 h at RT. 3,3′,5,5′-tetramethylbenzidine (TMB, Kem-En-Tec, cat# 4395L) was added, and the reaction stopped with 0.2 M H_2SO_4, followed by absorbance measurement at 450 nm (sample signal) and 655 nm (background signal) on a Clariostar plate reader (BMG Labtech, Ortenberg, Germany). The data was analyzed using GraphPad Prism 9.3.1 using 4PL fitting of dilution series, negative control samples too low to interpolate were set to limit of detection (LoD)/sqrt(2).[32]

5.7. *In Vivo* Circulatory Half-Life of Biomolecular Assemblies. Animal experiments were performed at the Department of Biomedicine, Aarhus University, under the Danish Animal Experiment Inspectorate license #2022−15−0201−01320 with ethical approval in accordance with the national guidelines for care and use of laboratory animals.

Male and female mice bearing both human FcRn and HSA genes ($hFcRn^{+/+}$, $hAlb^{+/+}$) controlled by an endogenous promoter were randomly divided into the following groups; rHA-HJ(EgA1, Cy5.5) (N = 4) and HJ(EgA1, Cy5.5) (N = 4). Three male mice were used as PBS control. 0.5 nmol in 50 μL of the assemblies or 50 μL PBS were administrated per 20 g mouse by intravenous tail vein injection with the amount scaled to the actual mouse weight.

Eighteen μL blood samples were collected from the tip of the tail vein in heparinized microcapillary tubes at 5 min and 1, 6, 24, and 48 h for rHA-HJ(EgA1, Cy5.5) and 5 and 30 min and 2, 6, and 24 h for HJ(EgA1, Cy5.5) post-injection. The collected blood was imaged after sampling in an Amersham Typhoon 5 (Cytiva). Data was analyzed in GraphPad Prism software v9.4.1. by a one-phase exponential decay model.

5.8. EGFR Binding of Biomolecular Assemblies using Flow Cytometry. For each sample, 100,000 3T3-EGFR or 150,000 3T3 or A431 cells were seeded in a 48-well plate and grown overnight at 37 °C, 5% CO_2. The medium was aspirated, and 25 nM samples in culturing medium were incubated with the cells for 30 min at 37 °C, 5% CO_2 before washing three times with DPBS and detaching cells with 0.25% trypsin/EDTA (Gibco, cat# 25200−056). Culturing medium was added to stop trypsinization, and the cells were washed and suspended in DPBS for analysis on a Novocyte flow cytometer (Agilent Technologies, Santa Clara, USA) using a 640 nm laser and 660/20 nm filter setting. Data was analyzed

https://doi.org/10.1021/acs.bioconjchem.3c00491
Bioconjugate Chem. 2024, 35, 214−222

using NovoExpress v. 1.2.5 (Agilent Technologies) and the gating strategy is shown in Figure S5.

■ ASSOCIATED CONTENT

Data Availability Statement

The data that support the findings of this study are available from the corresponding author upon reasonable request.

Supporting Information

The Supporting Information is available free of charge at https://pubs.acs.org/doi/10.1021/acs.bioconjchem.3c00491.

Purification of rHA-Q2 and Q1-EgA1, validation of EGFR expression in investigated cell lines, serum stability, and flow cytometry gating (PDF)

■ AUTHOR INFORMATION

Corresponding Author

Kenneth A. Howard − *Interdisciplinary Nanoscience Center (iNANO) and Department of Molecular Biology and Genetics, Aarhus University, DK-8000 Aarhus C, Denmark;* orcid.org/0000-0002-9407-278X; Email: kenh@inano.au.dk

Authors

Anders Dinesen − *Interdisciplinary Nanoscience Center (iNANO) and Department of Molecular Biology and Genetics, Aarhus University, DK-8000 Aarhus C, Denmark*

Veronica L. Andersen − *Interdisciplinary Nanoscience Center (iNANO) and Department of Molecular Biology and Genetics, Aarhus University, DK-8000 Aarhus C, Denmark*

Marwa Elkhashab − *Interdisciplinary Nanoscience Center (iNANO) and Department of Molecular Biology and Genetics, Aarhus University, DK-8000 Aarhus C, Denmark*

Diego Pilati − *Interdisciplinary Nanoscience Center (iNANO) and Department of Molecular Biology and Genetics, Aarhus University, DK-8000 Aarhus C, Denmark*

Pernille Bech − *Interdisciplinary Nanoscience Center (iNANO) and Department of Molecular Biology and Genetics, Aarhus University, DK-8000 Aarhus C, Denmark*

Elisabeth Fuchs − *Interdisciplinary Nanoscience Center (iNANO) and Department of Molecular Biology and Genetics, Aarhus University, DK-8000 Aarhus C, Denmark;* orcid.org/0000-0001-7450-754X

Torbjørn R. Samuelsen − *Interdisciplinary Nanoscience Center (iNANO) and Department of Molecular Biology and Genetics, Aarhus University, DK-8000 Aarhus C, Denmark*

Alexander Winther − *Interdisciplinary Nanoscience Center (iNANO) and Department of Molecular Biology and Genetics, Aarhus University, DK-8000 Aarhus C, Denmark*

Yunpeng Cai − *Interdisciplinary Nanoscience Center (iNANO) and Department of Molecular Biology and Genetics, Aarhus University, DK-8000 Aarhus C, Denmark*

Anders Märcher − *Interdisciplinary Nanoscience Center (iNANO) and Department of Chemistry, Aarhus University, DK-8000 Aarhus C, Denmark*

Archie Wall − *Department of Chemistry, University College London, London WC1H 0AJ, U.K.*

Marjan Omer − *Interdisciplinary Nanoscience Center (iNANO) and Department of Molecular Biology and Genetics, Aarhus University, DK-8000 Aarhus C, Denmark*

Jesper S. Nielsen − *Interdisciplinary Nanoscience Center (iNANO) and Department of Molecular Biology and Genetics, Aarhus University, DK-8000 Aarhus C, Denmark*

Vijay Chudasama − *Department of Chemistry, University College London, London WC1H 0AJ, U.K.;* orcid.org/0000-0002-8876-3285

James R. Baker − *Department of Chemistry, University College London, London WC1H 0AJ, U.K.;* orcid.org/0000-0002-7223-2279

Kurt V. Gothelf − *Interdisciplinary Nanoscience Center (iNANO) and Department of Chemistry, Aarhus University, DK-8000 Aarhus C, Denmark;* orcid.org/0000-0003-2399-3757

Jesper Wengel − *Nucleic Acid Center, Department of Physics, Chemistry, and Pharmacy, University of Southern Denmark, DK-5230 Odense M, Denmark;* orcid.org/0000-0001-9835-1009

Jørgen Kjems − *Interdisciplinary Nanoscience Center (iNANO) and Department of Molecular Biology and Genetics, Aarhus University, DK-8000 Aarhus C, Denmark;* orcid.org/0000-0003-4128-9317

Complete contact information is available at: https://pubs.acs.org/10.1021/acs.bioconjchem.3c00491

Notes

The authors declare no competing financial interest.

■ ACKNOWLEDGMENTS

This research was funded by the Novo Nordisk Foundation, Grant; CEMBID (Center for Multifunctional Biomolecular Drug Design, Grant Number: NNF17OC0028070) and the Villum Fonden, Grant; BioNEC (Biomolecular Nanoscale Engineering Center, grant number: VKR18333). M.E. recieved funding from the European Union's Horizon 2020 research and innovation programme under the Marie Skłodowska Curie grant agreement No. 955335, and D.P. from Independent Research Fund Denmark, Technology and Production grant 9041-00151B. The authors also gratefully acknowledge EPSRC and Albumedix for funding of A. Wall. The 3T3 and 3T3-EGFR cell line were generously donated by Dr. Luis Alvarez-Vallina (12 de Octubre University Hospital, Madrid, Spain).

■ REFERENCES

(1) Al-Lazikani, B.; Banerji, U.; Workman, P. Combinatorial drug therapy for cancer in the post-genomic era. *Nature biotechnology* **2012**, *30* (7), 679−692.

(2) Bunka, D. H. J.; Stockley, P. G. Aptamers come of age − at last. *Nature Reviews Microbiology* **2006**, *4* (8), 588−596.

(3) Okholm, A. H.; Kjems, J. DNA nanovehicles and the biological barriers. *Adv. Drug Delivery Rev.* **2016**, *106* (Pt A), 183−191.

(4) Larsen, M. T.; Kuhlmann, M.; Hvam, M. L.; Howard, K. A. Albumin-based drug delivery: harnessing nature to cure disease. *Mol. Cell. Ther.* **2016**, *4*, 3.

(5) Pilati, D.; Howard, K. A. Albumin-based drug designs for pharmacokinetic modulation. *Expert opinion on drug metabolism & toxicology* **2020**, *16* (9), 783−795.

(6) Schmidt, E. G. W.; Hvam, M. L.; Antunes, F.; Cameron, J.; Viuff, D.; Andersen, B.; Kristensen, N. N.; Howard, K. A. Direct demonstration of a neonatal Fc receptor (FcRn)-driven endosomal sorting pathway for cellular recycling of albumin. *J. Biol. Chem.* **2017**, *292* (32), 13312−13322.

(7) Chaudhury, C.; Mehnaz, S.; Robinson, J. M.; Hayton, W. L.; Pearl, D. K.; Roopenian, D. C.; Anderson, C. L. The major histocompatibility complex-related Fc receptor for IgG (FcRn) binds albumin and prolongs its lifespan. *J. Exp Med.* **2003**, *197* (3), 315−322.

(8) Matsumura, Y.; Maeda, H. A new concept for macromolecular therapeutics in cancer chemotherapy: mechanism of tumoritropic accumulation of proteins and the antitumor agent smancs. *Cancer research* **1986**, *46* (12 Pt 1), 6387−6392.
(9) Larsen, M. T.; Mandrup, O. A.; Schelde, K. K.; Luo, Y.; Sørensen, K. D.; Dagnæs-Hansen, F.; Cameron, J.; Stougaard, M.; Steiniche, T.; Howard, K. A. FcRn overexpression in human cancer drives albumin recycling and cell growth; a mechanistic basis for exploitation in targeted albumin-drug designs. *J. Controlled Release* **2020**, *322*, 53−63.
(10) Kuhlmann, M.; Hamming, J. B. R.; Voldum, A.; Tsakiridou, G.; Larsen, M. T.; Schmokel, J. S.; Sohn, E.; Bienk, K.; Schaffert, D.; Sorensen, E. S.; Wengel, J.; Dupont, D. M.; Howard, K. A. An Albumin-Oligonucleotide Assembly for Potential Combinatorial Drug Delivery and Half-Life Extension Applications. *Mol. Ther Nucleic Acids* **2017**, *9*, 284−293.
(11) Dinesen, A.; Winther, A.; Wall, A.; Märcher, A.; Palmfeldt, J.; Chudasama, V.; Wengel, J.; Gothelf, K. V.; Baker, J. R.; Howard, K. A. Albumin Biomolecular Drug Designs Stabilized through Improved Thiol Conjugation and a Modular Locked Nucleic Acid Functionalized Assembly. *Bioconjugate Chem.* **2022**, *33* (2), 333−342.
(12) Andersen, J. T.; Dalhus, B.; Cameron, J.; Daba, M. B.; Plumridge, A.; Evans, L.; Brennan, S. O.; Gunnarsen, K. S.; Bjørås, M.; Sleep, D.; Sandlie, I. Structure-based mutagenesis reveals the albumin-binding site of the neonatal Fc receptor. *Nat. Commun.* **2012**, *3* (1), 610.
(13) Andersen, V. L.; Vinther, M.; Kumar, R.; Ries, A.; Wengel, J.; Nielsen, J. S.; Kjems, J. A self-assembled, modular nucleic acid-based nanoscaffold for multivalent theranostic medicine. *Theranostics* **2019**, *9* (9), 2662−2677.
(14) Hofman, E. G.; Ruonala, M. O.; Bader, A. N.; van den Heuvel, D.; Voortman, J.; Roovers, R. C.; Verkleij, A. J.; Gerritsen, H. C.; van Bergen en Henegouwen, P. M. P. EGF induces coalescence of different lipid rafts. *J. Cell Sci.* **2008**, *121* (Pt 15), 2519−2528.
(15) Schmitz, K. R.; Bagchi, A.; Roovers, R. C.; Van Bergen en Henegouwen, P. M.; Ferguson, K. M. Structural evaluation of EGFR inhibition mechanisms for nanobodies/VHH domains. *Structure (London, England: 1993)* **2013**, *21* (7), 1214−1224.
(16) Teodori, L.; Omer, M.; Märcher, A.; Skaanning, M. K.; Andersen, V. L.; Nielsen, J. S.; Oldenburg, E.; Lin, Y.; Gothelf, K. V.; Kjems, J. Site-specific nanobody-oligonucleotide conjugation for super-resolution imaging. *J. Biol. Methods* **2022**, *9* (1), No. e159.
(17) Viuff, D.; Antunes, F.; Evans, L.; Cameron, J.; Dyrnesli, H.; Thue Ravn, B.; Stougaard, M.; Thiam, K.; Andersen, B.; Kjærulff, S.; Howard, K. A. Generation of a double transgenic humanized neonatal Fc receptor (FcRn)/albumin mouse to study the pharmacokinetics of albumin-linked drugs. *J. Controlled Release* **2016**, *223*, 22−30.
(18) Tedaldi, L. M.; Smith, M. E.; Nathani, R. I.; Baker, J. R. Bromomaleimides: new reagents for the selective and reversible modification of cysteine. *Chemical communications (Cambridge, England)* **2009**, *43*, 6583−6585.
(19) Wall, A.; Nicholls, K.; Caspersen, M. B.; Skrivergaard, S.; Howard, K. A.; Karu, K.; Chudasama, V.; Baker, J. R. Optimised approach to albumin-drug conjugates using monobromomaleimide-C-2 linkers. *Organic & biomolecular chemistry* **2019**, *17* (34), 7870−7873.
(20) Mandrup, O. A.; Ong, S. C.; Lykkemark, S.; Dinesen, A.; Rudnik-Jansen, I.; Dagnæs-Hansen, N. F.; Andersen, J. T.; Alvarez-Vallina, L.; Howard, K. A. Programmable half-life and anti-tumour effects of bispecific T-cell engager-albumin fusions with tuned FcRn affinity. *Commun. Biol.* **2021**, *4* (1), 310.
(21) Roopenian, D. C.; Low, B. E.; Christianson, G. J.; Proetzel, G.; Sproule, T. J.; Wiles, M. V. Albumin-deficient mouse models for studying metabolism of human albumin and pharmacokinetics of albumin-based drugs. *mAbs* **2015**, *7* (2), 344−351.
(22) Ibrahim, M.; Ramadan, E.; Elsadek, N. E.; Emam, S. E.; Shimizu, T.; Ando, H.; Ishima, Y.; Elgarhy, O. H.; Sarhan, H. A.; Hussein, A. K.; Ishida, T. Polyethylene glycol (PEG): The nature, immunogenicity, and role in the hypersensitivity of PEGylated products. *J. Controlled Release* **2022**, *351*, 215−230.
(23) Andersen, J. T.; Dalhus, B.; Viuff, D.; Ravn, B. T.; Gunnarsen, K. S.; Plumridge, A.; Bunting, K.; Antunes, F.; Williamson, R.; Athwal, S.; Allan, E.; Evans, L.; Bjørås, M.; Kjærulff, S.; Sleep, D.; Sandlie, I.; Cameron, J. Extending serum half-life of albumin by engineering neonatal Fc receptor (FcRn) binding. *J. Biol. Chem.* **2014**, *289* (19), 13492−13502.
(24) Larsen, M. T.; Rawsthorne, H.; Schelde, K. K.; Dagnaes-Hansen, F.; Cameron, J.; Howard, K. A. Cellular recycling-driven in vivo half-life extension using recombinant albumin fusions tuned for neonatal Fc receptor (FcRn) engagement. *J. Controlled Release* **2018**, *287*, 132−141.
(25) Singh, S. K.; Koshkin, A. A.; Wengel, J.; Nielsen, P. LNA (locked nucleic acids): synthesis and high-affinity nucleic acid recognition. *Chem. Commun.* **1998**, *4*, 455−456.
(26) Obika, S.; Nanbu, D.; Hari, Y.; Andoh, J.-i.; Morio, K.-i.; Doi, T.; Imanishi, T. Stability and structural features of the duplexes containing nucleoside analogues with a fixed N-type conformation, 2′-O,4′-C-methyleneribonucleosides. *Tetrahedron Lett.* **1998**, *39* (30), 5401−5404.
(27) Märcher, A.; Kumar, V.; Andersen, V. L.; El-Chami, K.; Nguyen, T. J. D.; Skaanning, M. K.; Rudnik-Jansen, I.; Nielsen, J. S.; Howard, K. A.; Kjems, J.; Gothelf, K. V. Functionalized Acyclic (l)-Threoninol Nucleic Acid Four-Way Junction with High Stability In Vitro and In Vivo. *Angew. Chem., Int. Ed.* **2022**, *61* (24), No. e202115275.
(28) Yarden, Y.; Pines, G. The ERBB network: at last, cancer therapy meets systems biology. *Nature Reviews Cancer* **2012**, *12* (8), 553−563.
(29) Rudnik-Jansen, I.; Howard, K. A. FcRn expression in cancer: Mechanistic basis and therapeutic opportunities. *J. Controlled Release* **2021**, *337*, 248−257.
(30) Zanetti-Domingues, L. C.; Korovesis, D.; Needham, S. R.; Tynan, C. J.; Sagawa, S.; Roberts, S. K.; Kuzmanic, A.; Ortiz-Zapater, E.; Jain, P.; Roovers, R. C.; Lajevardipour, A.; van Bergen en Henegouwen, P. M. P.; Santis, G.; Clayton, A. H. A.; Clarke, D. T.; Gervasio, F. L.; Shan, Y.; Shaw, D. E.; Rolfe, D. J.; Parker, P. J.; Martin-Fernandez, M. L. The architecture of EGFR's basal complexes reveals autoinhibition mechanisms in dimers and oligomers. *Nat. Commun.* **2018**, *9* (1), 4325.
(31) Chatterjee, A.; Sun, S. B.; Furman, J. L.; Xiao, H.; Schultz, P. G. A Versatile Platform for Single- and Multiple-Unnatural Amino Acid Mutagenesis in Escherichia coli. *Biochemistry* **2013**, *52* (10), 1828−1837.
(32) Armbruster, D. A.; Pry, T. Limit of blank, limit of detection and limit of quantitation. *Clin. Biochemist. Rev.* **2008**, *29 Suppl 1* (Suppl 1), S49−52.

https://doi.org/10.1021/acs.bioconjchem.3c00491
Bioconjugate Chem. 2024, 35, 214−222